UDC 539.4

Numerical Simulation of Elastic Linear Micropolar Media Based on the Pore Space Length Scale Assumption

J. Jeong, H. Adib-Ramezani, and M. Al-Mukhtar

École Polytechnique de l'Université d'Orléans, Orléans, France

УДК 539.4

Численное моделирование линейно-упругой микрополярной среды на основе анализа характерного размера микропор

Ж. Жеонг, Х. Адиб-Рамезани, М. Аль-Мухтар

Политехнический институт Орлеанского университета, Орлеан, Франция

В рамках трехмерной микрополярной теории выполнено численное моделирование хрупких изотропных материалов с различными размерами пор (аморфное стекло, хрупкая скальная порода и два различных типа легкого бетона) с использованием цилиндрических моделей при воздействии одноосной сжимающей нагрузки. Для решения задачи предполагается, что первая, вторая и третья константы микровращения (α, β и γ) в уравнении баланса напряжений пропорциональны квадрату среднего диаметра поры или так называемой характерной длины. Оказалось, что такое допущение приводит к постоянству полярного коэффициента Ψ и, следовательно, он не может трактоваться как константа материала. Это может служить основанием для введения дополнительной константы материала для трехмерных микрополярных сред. Соответственно константа микрополярного сдвига κ является константой материала, что противоречит новейшим результатам. Выполнены численные расчеты для различных значений степеней свободы N и соответствующих областей с целью исследования характерных особенностей константы микрополярного сдвига κ. С использованием предложенной методики установлена хорошая сходимость и совместимость полученных данных с экспериментальными для разнородных и однородных материалов с нано- и микропорами, в то время как для пор мезомасштаба получен ряд непреобразуемых или прерывистых полей напряжений.

Ключевые слова: микрополярная теория, численное моделирование, хрупкие материалы, константы материала, характерная длина.

Notation

u_i – small displacements
φ_i – microrotations
e_{ijk} – permutation tensor
ω_i – rotation fields (macrorotation)
σ_{ij} – stress tensor
k_{ij} – curvature tensor
m_{ij} – couple stress tensor
γ_{ij} – small strain tensor

ε_{ij} – symmetric part of small strain tensor γ_{ij}
β_{ij} – antisymmetric part of small strain tensor γ_{ij}
δ_{ij} – Kronecker delta
λ', μ', κ' – material constants
λ – first Lame's constant
μ – second Lame's constant
κ – micropolar shear constant
α – first microrotation constant
β – second microrotation constant
γ – third microrotation constant
t_i – surface traction
Q_i – surface couple
n_i – unit outward vector normal to the surface S
Ψ – polar ratio
N – coupling number
l_t – characteristic length for torsion
l_b – characteristic length for bending
l_1 – first characteristic length scale
l_2 – second characteristic length scale
l_3 – third characteristic length scale
l_G – characteristic length or average pore diameter
Ω – field equations
Ω_i – boundary condition settings
σ_0 – applied compressive loading

Introduction. After the work of Cosserat's brothers [1], the micropolar theory has been followed and completed by other authors [2–13]. This theory has been evolved into the micromorphic theory later. The micromorphic materials contain the "stress moments" and "body moments," and they are affected by the spin inertia [3–6]. Thus, there are three constitutive equations, which are stress tensor, microstress tensor, and first stress moment ones, with 18 material constants.

The general micromorphic theory is usually complicated for the mathematical analyses and applications. Eringen has introduced the antisymmetric (skew symmetric) properties for first stress moment and microrotation for the simplification of that theory [3–6]. Such a simplified theory enables one to treat physically realistic problems and make completely feasible the mathematical applications. The assumptions introduced by Eringen lead to a micropolar theory in which two constitutive equations (stress and couple stress) with 6 material constants can be found.

A further simplified micropolar theory can be obtained assuming that macrorotations are the same as microrotations, which is named "couple stress theory" [7–9]. The concept of micropolar theory involves the microstructures into the continuum media (Fig. 1).

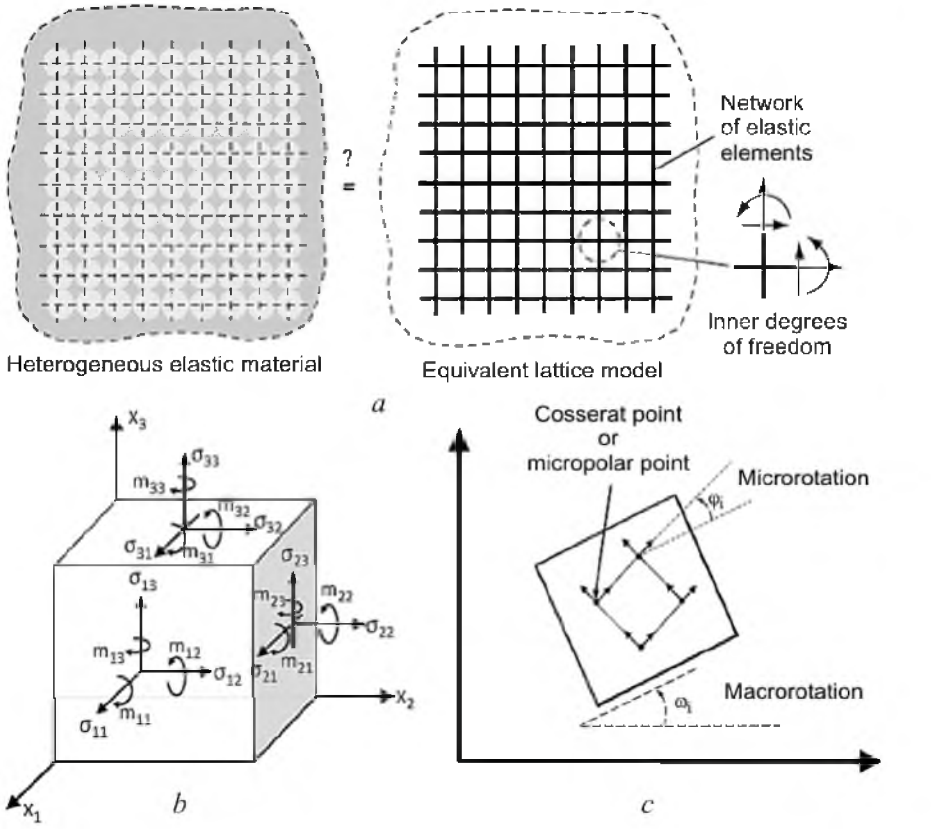

Fig. 1. Modeling of heterogeneous materials with microstructure [14] (*a*), components of stress and couple stress tensors for micropolar solids (*b*), microrotation compared to macrorotation (*c*).

This theory can explain and analyze more efficiently the diagonal fracture plane under compressive loading for heterogeneous materials, e.g., sand, soil, and high porous rock, than the classical continuum theory [15–18]. It is noteworthy, that the other theories can also provide the microrotations of particles and their localizations on the shear bands via the 2D numerical methods [19, 20]. Unfortunately, the direct measurements of microrotation of particles are not achievable with high accuracy but we can measure the displacements in the diagonal fracture plane by means of stereophotometric method [21].

The micropolar theory can be also used as a generalized continuum theory in which microstructure detail can be averaged out by the "characteristic length scale" [22–24]. This last parameter can be considered as the smallest homogeneous region in heterogonous media and it is frequently used to model the damage phenomenon in concrete [25, 26].

The main problem of the micropolar theory is to determine "precisely" the material constants using experiments, which is not always easy to achieve. Lakes [10–12] proposed an experimental procedure to find out four supplementary material constants (κ, α, β, and γ) for micropolar media but it is difficult and not achievable for all heterogeneous materials in reality. The choice of the material constants remains not enough precise and clear due to the difficulty of experiments and some assumptions in the proposed relations [27–29].

The goal of this paper is to improve our last numerical study in micropolar theory [30] and to investigate the characteristic length scale based on the pore size influence on the mechanical behavior using the developed analytical relations for the 3D micropolar theory. The analytical estimations are used to evaluate the material constants using the strain-energy density positive definiteness postulate. Moreover, the results are compared to the classical continuum media or Cauchy's media with the identical loading, geometry and mechanical properties. Indeed, the strain-energy density value is considered the same for micropolar and Cauchy cases. The above-mentioned analysis should be applicable to both heterogeneous and homogeneous materials in a unified methodology. To pursue this objective, four different brittle materials are considered. The first material is an amorphous material with very low porosity and nanoscale pore size (glass [31]), second material is a heterogeneous material with high porosity and the microscale pore size (sedimentary rock [32]), and the two last materials are porous and lightweight concretes [33] with different porosities and the mesoscale pores. The mentioned elastic brittle materials are analyzed in order to evaluate the average pore size as the characteristic length scale in micropolar theory, and the findings are compared to the Cauchy's theory results. Finally, the numerical results clarify the material constant nature of micropolar theory and average pore size effect for three-dimensional models and its role in the mechanical behavior of the considered materials. It is important to state that the three-dimensional micropolar models require six material constants, while the two-dimensional micropolar models need only four material constants. Accordingly, the three-dimensional numerical analyses are always more complicated than the two-dimensional models, which are commonly used to elucidate and delineate the shear localization phenomenon.

1. **Mathematical Formulation of Micropolar Solids**. For a linear elastic anisotropic micropolar solid, a strain-energy density function W can be expressed as a polynomial in function of γ_{ij} and k_{ij} based on the expansion power series theory [34],

$$W(\gamma_{ij}, k_{ij}) = A_0 + A_{ij}\gamma_{ij} + B_{ij}k_{ij} + C_{ijkl}\gamma_{ij}k_{kl} + \frac{1}{2}D_{ijkl}\gamma_{ij}\gamma_{kl} + \frac{1}{2}E_{ijkl}k_{ij}k_{kl} \qquad \text{for} \qquad i, j, k, l = 1, 2, 3, \tag{1}$$

where γ_{ij} is the small strain tensor, which composes the symmetric ε_{ij} and antisymmetric parts β_{ij}, and k_{ij} is the curvature tensor. In the absence of initial stress and couple stress ($A_0 = A_{ij} = B_{ij} = 0$) and the hypothesis of centrosymmetry coefficient of micropolar media ($C_{ijkl}0$), we can find the following constitutive equations:

$$\begin{cases} \sigma_{ij} = \dfrac{\partial W}{\partial \gamma_{ij}} = D_{ijkl}\gamma_{kl}, \\ m_{ij} = \dfrac{\partial W}{\partial k_{ij}} = E_{ijkl}k_{kl}, \end{cases} \qquad \text{for} \qquad i, j, k, l = 1, 2, 3, \tag{2}$$

where the fourth order stiffness tensors D_{ijkl} and E_{ijkl} have the symmetry properties.

Using the above-mentioned property and isotropy of the fourth order stiffness tensors, the constitutive equations in Eq. (2) can be rewritten as follows [34]:

$$\begin{cases} \sigma_{ij} = \lambda\gamma_{kk}\delta_{ij} + (\mu+\kappa)\gamma_{ij} + (\mu-\kappa)\gamma_{ij}, \\ m_{ij} = \lambda' k_{kk}\delta_{ij} + (\mu'+\kappa')k_{ij} + (\mu'-\kappa')k_{ij}, \end{cases} \quad \text{for} \quad i, j, k = 1, 2, 3. \tag{3}$$

The kinematic relation in micropolar media is

$$\gamma_{ij} = \varepsilon_{ij} + \beta_{ij} = u_{j,i} - e_{kij}\varphi_k \qquad \text{for} \qquad i, j, k = 1, 2, 3, \tag{4}$$

$$k_{ij} = \varphi_{j,i} \qquad \text{for} \qquad i, j = 1, 2, 3, \tag{5}$$

where e_{kij} is the permutation tensor,

$$\varepsilon_{ij} = \frac{1}{2}(u_{i,j} + u_{j,i}), \qquad \beta_{ij} = e_{ijk}(\omega_k - \varphi_k) \qquad \text{for} \qquad i, j, k = 1, 2, 3, \tag{6}$$

where ε_{ij}, β_{ij}, u_i, and φ_k are symmetric part of γ_{ij} or small strain tensor, antisymmetric part of γ_{ij}, displacement fields and the microrotation fields, respectively. The classical macrorotations ω_k can be described as follows:

$$\omega_i = \frac{1}{2}e_{ijk}u_{k,j} \qquad \text{for} \qquad i, j, k = 1, 2, 3. \tag{7}$$

It is assumed that the rotation field (macrorotation) is kinematically independent from the displacement field and φ_i is distinct from the material rotation. Within framework of the micropolar continuum theory, not only forces but also moments can be transmitted across the surface of a material element. The kinematical considerations for micropolar and Cauchy's theory are identical for small displacement but micropolar theory has three additional dependent variables (φ_i) in respect to the Cauchy's one (u_i).

According to the microrotations in the micropolar theory, the gradient of the rotation vector can be added and defined as the curvature tensor k_{ij}, which is related by a constitutive relation to the couple stress tensor m_{ij}. With substitution of the equations (4) and (5) into the equation (3), the constitutive equations can be rewritten as

$$\begin{cases} \sigma_{kl} = \lambda\varepsilon_{rr}\delta_{kl} + (2\mu+\kappa)\varepsilon_{kl} + \kappa e_{klm}(\omega_m - \varphi_m), \\ m_{kl} = \alpha\varphi_{r,r}\delta_{kl} + \beta\varphi_{k,l} + \gamma\varphi_{l,k}, \end{cases} \quad \text{for} \quad k, l, m, r = 1, 2, 3, \tag{8}$$

where δ_{kl} is the Kronecker symbol, λ and μ are the classical Lame's constants, κ, α, β, and γ are new material constants introduced in micropolar theory. The

positive definiteness of the strain-energy density requires some restrictions on the micropolar constants,

$$\begin{cases} \mu > 0, & 3\lambda + 2\mu > 0, \quad \beta > 0, \quad 3\alpha + 2\beta > 0, \\ \mu + \kappa > 0, & \beta + \gamma > 0, \quad \kappa > 0, \quad \gamma > 0. \end{cases} \tag{9}$$

In the absence of body forces and body couples, the equilibrium equations of the micropolar theory are given as

$$\begin{cases} \sigma_{ji,j} = 0, \\ m_{ji,j} = e_{ijk}\sigma_{jk}, \end{cases} \quad \text{for} \quad i, j, k = 1, 2, 3. \tag{10}$$

The Eq. (10) implies that the Cauchy stress tensor σ_{ji} is not necessarily symmetric and its antisymmetric part is determined by the divergence of the couple stress tensor m_{ji}. According to the minimum total potential energy principal, the relation between the variational elastic strain-energy density and the potential energy function of the body having volume V and surface S for micropolar is denoted by

$$\iiint_V (\sigma_{ij}\delta\gamma_{ij} + m_{ij}\delta k_{ij})dV = \iint_S (t_i\delta u_i + Q_i\delta\varphi_i)dS \quad \text{for} \quad i, j = 1, 2, 3, \tag{11}$$

where t_i is the surface traction and Q_i is the surface couple, and they can be denoted as follows:

$$t_i = \sigma_{ji}n_j \quad \text{and} \quad Q_i = m_{ji}n_j \quad \text{for} \quad i, j = 1, 2, 3, \tag{12}$$

where n_j is the unit outward vector normal to the surface S. Alternatively, the variational elastic strain-energy density for Cauchy's media can be described as

$$\iiint_V (\sigma_{ij}\delta\varepsilon_{ij})dV = \iint_S (t_i\delta u_i)dS \quad \text{for} \quad i, j = 1, 2, 3. \tag{13}$$

It is noteworthy, that for the same geometrical configuration and loading application, the micropolar normal stress components are smaller than those found by the Cauchy ones. Accordingly, the micropolar shear stress components are greater than those found by the Cauchy ones. The comparison of several terms in Eqs. (11) and (13) can substantiate these differences under equality of right hand sides of Eqs. (11) and (13):

$$\overbrace{\iiint_V (\sigma_{ij}\delta\gamma_{ij} + m_{ij}\delta k_{ij})dV}^{\text{micropolar media}} = \overbrace{\iiint_V (\sigma_{ij}\delta\varepsilon_{ij})dV}^{\text{Cauchy's media}} \quad \text{for} \quad i, j = 1, 2, 3. \tag{14}$$

Therefore, due to the micropolar theory assumptions, the shear stress components variations control couple stress tensor m_{ij}.

2. **Analytical Evaluation of the Material Constants in Micropolar Theory and Characteristic Length**. The four supplementary material constants for three-dimensional analysis, κ, α, β, and γ can be expressed by the four new terms, Ψ, N, l_t, and l_b, the polar ratio, coupling number, characteristic length for torsion and bending according to Lakes [10–13, 35] (Table 1).

T a b l e 1

Material Constants in Micropolar Theory [10–13, 35]

Material constants	Engineering constants	Continuum mechanics constants
Young's modulus	$E=\dfrac{(2\mu+\kappa)(3\lambda+2\mu+\kappa)}{2\lambda+2\mu+\kappa}$	$\lambda=\dfrac{\nu E}{(1+\nu)(1-2\nu)}$
Shear modulus	$G=\dfrac{2\mu+\kappa}{2}$	$\mu=\dfrac{(1-2N^2)G}{1-N^2}$
Poisson's ratio	$\nu=\dfrac{\lambda}{2\lambda+2\mu+\kappa}$	$G=\dfrac{E}{2(1+\nu)}$
Characteristic length for rotation	$l_t=\left(\dfrac{\beta+\gamma}{2\mu+\kappa}\right)^{0.5}$	$\kappa=\dfrac{2N^2G}{1-N^2}$
Characteristic length for bending	$l_b=\left(\dfrac{\gamma}{2(2\mu+\kappa)}\right)^{0.5}$	$\alpha=\dfrac{2(1-\Psi)Gl_t^2}{\Psi}$
Coupling number	$N=\left(\dfrac{\kappa}{2(\mu+\kappa)}\right)^{0.5}$, $0\le N\le 1$	$\beta=2G(l_t^2-2l_b^2)$
Polar ratio	$\Psi=\dfrac{\beta+\gamma}{\alpha+\beta+\gamma}$, $0\le\Psi\le 1.5$	$\gamma=4Gl_b^2$

When κ, α, β, and γ vanish, the solid body becomes classically elastic. In Table 1, $\kappa=0$ signifies that the coupling number, N becomes zero and the shear modulus (μ) is identical to the classical continuum theory (G). The mentioned case corresponds to a decoupling of the rotational and translational degrees of freedom [10–12]. However, the recent work [2] highlights that the value κ, is not a material constant, it can be set to zero.

If $\kappa\to\infty$, the classical elastic constants E, G, and ν are no more meaningful and the characteristic lengths (l_t, l_b) become zero and coupling number N is equal to one. This case is well known as "couple stress theory" [3, 7–9]. The latter case deals with that material is incompressible, i.e., the microrotation is assumed equal to the macrorotation throughout material body.

The first three material constants are analyzed and the graphical results concerning the relationship between the coupling number and the Poisson's ratios are illustrated in Fig. 2 [30].

The first Lame's material constant (λ) over shear modulus (G) versus Poisson's ratio is illustrated using auxiliary axis. As shown in Fig. 2, Poisson's ratio varies between -1 and 0.5. The value of Poisson's ratio changes between 0 and 0.5 for the classical materials except to some special materials. For the μ/G and

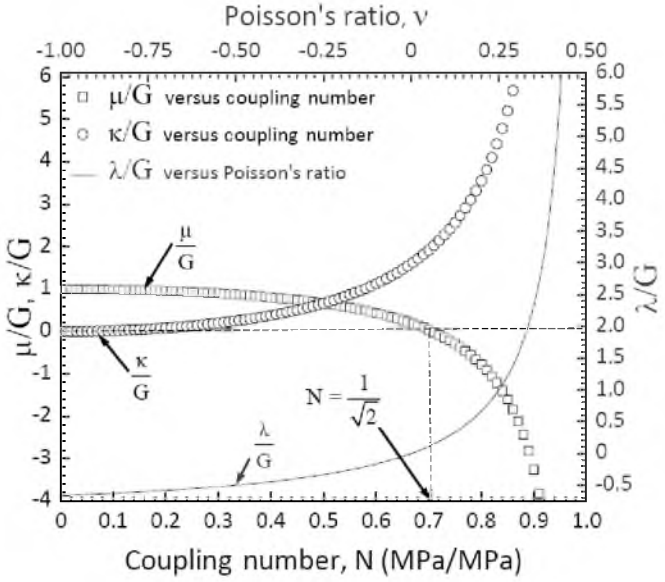

Fig. 2. Nondimensional micropolar isotropic elastic linear media material constants variation: μ/G and κ/G variations versus coupling number, $0 \le N \le 1$ and λ/G versus Poisson's ratio, $-1 \le \nu \le 0.5$ [30].

κ/G ratios, we find out high positive and negative values when the coupling number reaches its maximum value ($N = 1$).

In Fig. 3, the material constants for rotational aspects are deemed in conjunction with the torsion over bending characteristic length ratio (l_t/l_b) and polar ratio Ψ. As demonstrated in Fig. 3, $\gamma/2Gl_b^2$ is entirely constant and equal to two and $\beta/2Gl_b^2$ varies very slightly in function of the two characteristic lengths ratio. However, $\alpha/2Gl_b^2$ depends not only on the characteristic length ratio but also on the polar ratio Ψ: the $\alpha/2Gl_b^2$ value is more important if the polar ratio becomes less than 1, otherwise, the last value remains constant. Moreover, the polar ratio cannot exceed the value of 1.5 due to the thermodynamical laws [10]. Using the estimation of characteristic length based on the homogenization approach by Bigoni [36], the material constants can be calculated and the polar ratio Ψ does not affect the micro- and macrorotations for 3D micropolar theory simulations [30]. However, the problem is that the last obtained values cannot satisfy the definition of positive strain energy [Eq. (9)]. In this paper, we attempt to apply a more simplified and efficient methodology in which we can use the average pore diameter as characteristic length l_G. Furthermore, the mentioned graphical analysis (Fig. 3) permits us to use the characteristic length l_G which can efficiently simplify the micropolar constants (α, β, γ, l_t, and l_b). There are two distinct sets of moduli: μ, λ, and κ which relate the traditional stresses and strains and have a dimension of force per unit area, and α, β, and γ which relate to the higher-order couple-stresses and torsion, with a dimension of force. Due to the dimensional difference between the two sets of moduli, at least three intrinsic characteristic lengths can be defined for an isotropic elastic micropolar material. These characteristic lengths can be denoted as [8, 18]:

$$l_1 = (\gamma/\mu)^{1/2}, \qquad l_2 = (\beta/\mu)^{1/2}, \qquad l_3 = (\alpha/\mu)^{1/2}, \tag{15}$$

and the characteristic length l_G can be expressed as

$$l_1 = l_2 = l_3 = l_G = \text{average pore diameter}. \tag{16}$$

The constitutive equation [Eq. (8)] can be rewritten including the characteristic length l_G [Eqs. (15) and (16)] in following form:

$$\begin{cases} \sigma_{kl} = \lambda \varepsilon_{rr} \delta_{kl} + (2\mu + \kappa)\varepsilon_{kl} + \kappa e_{klm}(\omega_m - \varphi_m), \\ m_{kl} = l_G^2(\varphi_{r,r}\delta_{kl} + \varphi_{k,l} + \varphi_{l,k}), \end{cases} \quad \text{for} \quad k, l, m, r = 1, 2, 3. \tag{17}$$

The above definition [Eq. (17)] will be applied in the numerical simulation comparing between micropolar theory and Cauchy's approach on the brittle isotropic materials with different pore size in the next section.

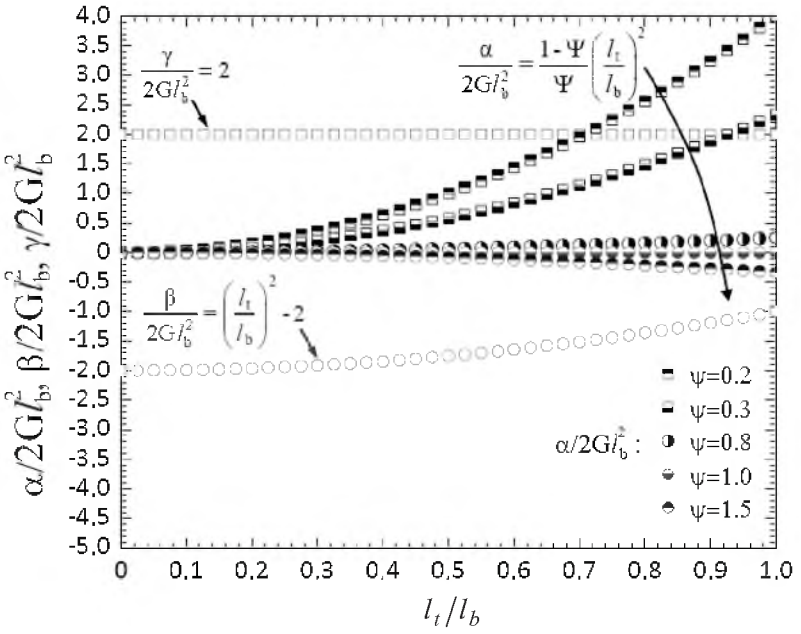

Fig. 3. Nondimensional micropolar isotropic elastic linear media material constants variation: $\alpha/2Gl_b^2$, $\beta/2Gl_b^2$, and $\gamma/2Gl_b^2$ variations versus torsion over bending characteristic length ratio for different polar ratios, $0 \le \Psi \le 1.5$ [30].

3. **Numerical Simulation of the Micropolar Theory**. We study four elastic brittle materials as glass material, high porous rock and two porous lightweight concretes with the same pore sizes and different modulus of elasticity with the same geometry subjected to the identical compressive loading. The geometry ($r = 20$ mm and $h = 80$ mm in Fig. 4) is chosen according to the AFNOR standard for the uniaxial compression experiments. The mechanical properties of these materials are summarized in Table 2.

Table 2

Material Constants of the Considered Brittle Materials

Material		E, GPa	ν	l_G, m	Coupling number N (see Table 1)	Polar ratio Ψ (see Table 1)
M1	Glass materials [31]	50	0.2	$1\cdot10^{-9}$	$0 \le N \le 1$	2/3
M2	Brittle rocks [32]	1	0.2	$5\cdot10^{-6}$	$0 \le N \le 1$	2/3
M3	Lightweight concrete 1 [33]	34	0.2	$1\cdot10^{-3}$	$0 \le N \le 1$	2/3
M4	Lightweight concrete 2 [33]	14	0.2	$1\cdot10^{-3}$	$0 \le N \le 1$	2/3

The constitutive equations of micropolar theory [Eq. (8)], kinematic relation [Eqs. (4)–(6)] can be introduced into the two equilibrium equations [Eq. (10)] to find out the so called "micropolar Navier's equation" excluding body force and body couple effects for the static state [Eq. (18)].

$$\begin{cases} \lambda u_{k,kj}\delta_{ij} + \mu(u_{i,jj} + u_{j,ij}) + \dfrac{\kappa}{2}(u_{i,jj} + u_{j,ij}) + \kappa e_{jik}\left(e_{klm}\dfrac{u_{m,lj}}{2} - \varphi_{k,j}\right) = 0, \\ \alpha\varphi_{k,kj}\delta_{ij} + \beta\varphi_{j,ij} + \gamma\varphi_{i,jj} + \lambda u_{k,kj}\delta_{ij} + \mu(u_{k,jj} + u_{j,kj}) + \\ + \dfrac{\kappa}{2}(u_{k,jj} + u_{j,kj}) + \kappa e_{jkr}\left(e_{rim}\dfrac{u_{m,l}}{2} - \varphi_r\right) = 0, \\ \text{for} \quad i, j, k, l, m, r = 1, 2, 3. \end{cases} \tag{18}$$

Using characteristic length l_G [Eqs. (15) and (16)], we can rewrite the equilibrium equations as

$$\Omega: \begin{cases} \dfrac{\lambda(u_{k,kj}\delta_{ij})}{\mu} + (u_{k,jj} + u_{j,kj}) + \dfrac{\kappa}{2\mu}(u_{k,jj} + u_{j,kj}) + \\ + \dfrac{\kappa e_{jkr}\left(e_{rim}\dfrac{u_{m,l}}{2} - \varphi_r\right)}{\mu} = 0, \\ l_G^2(\varphi_{k,k}\delta_{ij} + \varphi_{j,ij} + \varphi_{i,jj}) + (u_{k,jj} + u_{j,kj}) + \dfrac{\kappa}{2\mu}(u_{k,jj} + u_{j,kj}) + \\ + \dfrac{\kappa e_{jkr}\left(e_{rim}\dfrac{u_{m,l}}{2} - \varphi_r\right)}{\mu} = 0, \\ \text{for} \quad i, j, k, l, m, r = 1, 2, 3, \end{cases} \tag{19}$$

where u_i are small displacements and φ_i are the microrotations, λ, μ, and κ are the material constants in conjunction with the modulus of elasticity and shear

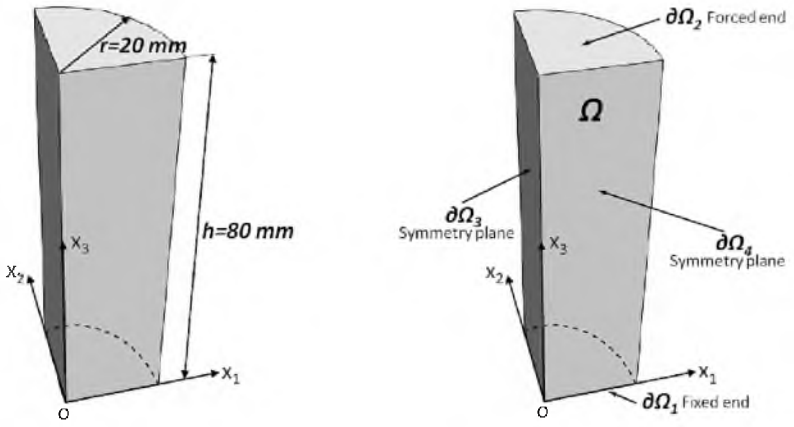

Fig. 4. Geometrical configuration and boundary condition for a quarter cylindrical models.

modulus (engineering material constants in Table 2), and l_G^2 signifies the state of the microstructure and pore size. In order to obtain the numerical solutions via micropolar theory for the above-mentioned materials, we solve the obtained partial differential equations (PDEs) of micropolar elasticity [Eq. (19)] for the cylindrical specimens under compressive loading by means of the corresponding boundary conditions [Eq. (20)]. The applied compressive stress is assumed to be equal to $\sigma_0 = 5$ MPa. The coupling number is varied from 0 to 0.7 for chosen materials (M1, M2, M3, and M4). The appropriate boundary conditions are presented in Eq. (20).

$$
\begin{aligned}
&\partial\Omega_1: \begin{cases} u_i = 0, \\ \varphi_i = 0, \end{cases} \quad \text{for} \quad i = 1, 2, 3, \\
&\partial\Omega_2: \begin{cases} \{t_i = \sigma_{ji} n_j = 0 \quad (i = 1, 2)\} \cup \{t_i = \sigma_{ji} n_j = -\sigma_0 \quad (i = 3)\} \quad \text{for} \quad j = 1, 2, 3, \\ Q_i = m_{ji} n_i = 0 \quad \text{for} \quad i, j = 1, 2, 3, \end{cases} \\
&\partial\Omega_3: \begin{cases} \{u_i = 0 \quad \text{for} \quad i = 1\} \cup \{u_i \neq 0 \quad \text{for} \quad i = 2, 3\}, \\ \varphi_i \neq 0 \quad \text{for} \quad i = 1, 2, 3, \end{cases} \\
&\partial\Omega_4: \begin{cases} \{u_i = 0 \quad \text{for} \quad i = 2\} \cup \{u_i \neq 0 \quad \text{for} \quad i = 1, 3\}, \\ \varphi_i \neq 0 \quad \text{for} \quad i = 1, 2, 3. \end{cases}
\end{aligned}
\tag{20}
$$

In Fig. 4, the geometrical configuration and boundary conditions are illustrated. The Ω symbol indicates the field equations for selected continuum media [Eq. (19)].

The $\partial\Omega_i$ symbols deal with the applied boundary conditions [Eq. (20)]. Due to the symmetry of geometry and loading, a quarter of cylindrical model and the required symmetrical boundary conditions are analyzed. This makes possible to obtain a higher mesh density for numerical calculations and more precise numerical Gauss integrations around the stress concentration zones. In Eq. 20, $\partial\Omega_1$ and $\partial\Omega_2$ deal with the fixed end and forced end, respectively. Indeed, we fix one end including displacements and microrotations and apply compressive

loading as an inward stress vector (σ_0). Hence, $\partial\Omega_1$ represents the Dirichlet boundary condition and $\partial\Omega_2$ signifies the Neumann boundary condition. In Eq. (20), $\partial\Omega_3$ and $\partial\Omega_4$ deal with the $x_2 - x_3$ symmetry plane and $x_1 - x_3$ symmetry plane, respectively. In the next section, Eq. (19) for the brittle materials (M1, M2, M3, and M4) will be solved using these boundary conditions [Eq. (20)]. The impact of coupling number N on the numerical models will be also investigated.

4. **Numerical Simulation Results and Discussion**. As illustrated in Fig. 2, the coupling number values N larger than $1/\sqrt{2}$ lead to the negative values for μ. According to the Eq. (9), the negative values are not feasible due to the positive definiteness of strain-energy density. Consequently, the coupling number values between 0 and $1/\sqrt{2}$ should be considered. Furthermore, the numerical calculations for $N = 0$ and $N = 1/\sqrt{2}$ yield the divergency of solution.

The numerical studies are restricted to $0.1 \le N \le 0.7$ in order to avoid the above-mentioned disadvantages. The compressive stress distribution and micro-rotation are calculated with the help of numerical solution with assumptions described in the previous section. The stress components (σ_{33}, σ_{31}) for the selected cylindrical geometry using micropolar and Cauchy media assumptions are shown in Fig. 5 for M2. The axial and shear stress distribution are similar to the Cauchy's one: it can be observed the stress concentration and microrotation concentration at the bottom and near the bottom due to the boundary conditions, respectively. As expected from the above results, less normal stress in longitudinal direction (σ_{33}) for micropolar media (Fig. 5*a*) is found out while the shear stress components are increased compared to the Cauchy's media (Fig. 5*d* and 5*e*). These facts can be explained using the equality of the strain-energy density concept [Eq. (14)]. In fact, the strain-energy densities for two cases are identical. The coupling number N was changed to observe the axial and shear stress distribution variation in this model for different characteristic length scales. The numerical results are described in Fig. 6.

Low shear stress value is obtained near the bottom of specimen or fixed end as expected. The couple stress values are found to be low because the couple stress tensor depends on shear stress due to the equilibrium equations [Eq. (10)] and consequently, low couple stress values can be extracted. In particular, the displacement and microrotation fields are emphasized. The stress and displacement are compared to the Cauchy's stress theory results for the purpose of evaluating and verifying the validity of the numerical calculations. The numerical results imply that N is related to the micropolar effects, and higher values of coupling number N intensify the shear stress impact on the stress distribution of the model considered here. The shear stress increase can be observed as a function of the coupling number value as shown in Fig. 6.

It is necessary to mention that coupling number variations imply different materials, i.e., we study different materials. The three-dimensional micropolar analysis assumptions result in six material constants. As previously discussed, the application of Eq. (15) reduces these material constants to four material constants (λ, μ, κ, and l_G). According to the presented relations in Table 1, it can be concluded that κ cannot be determined without one assumption about coupling number N.

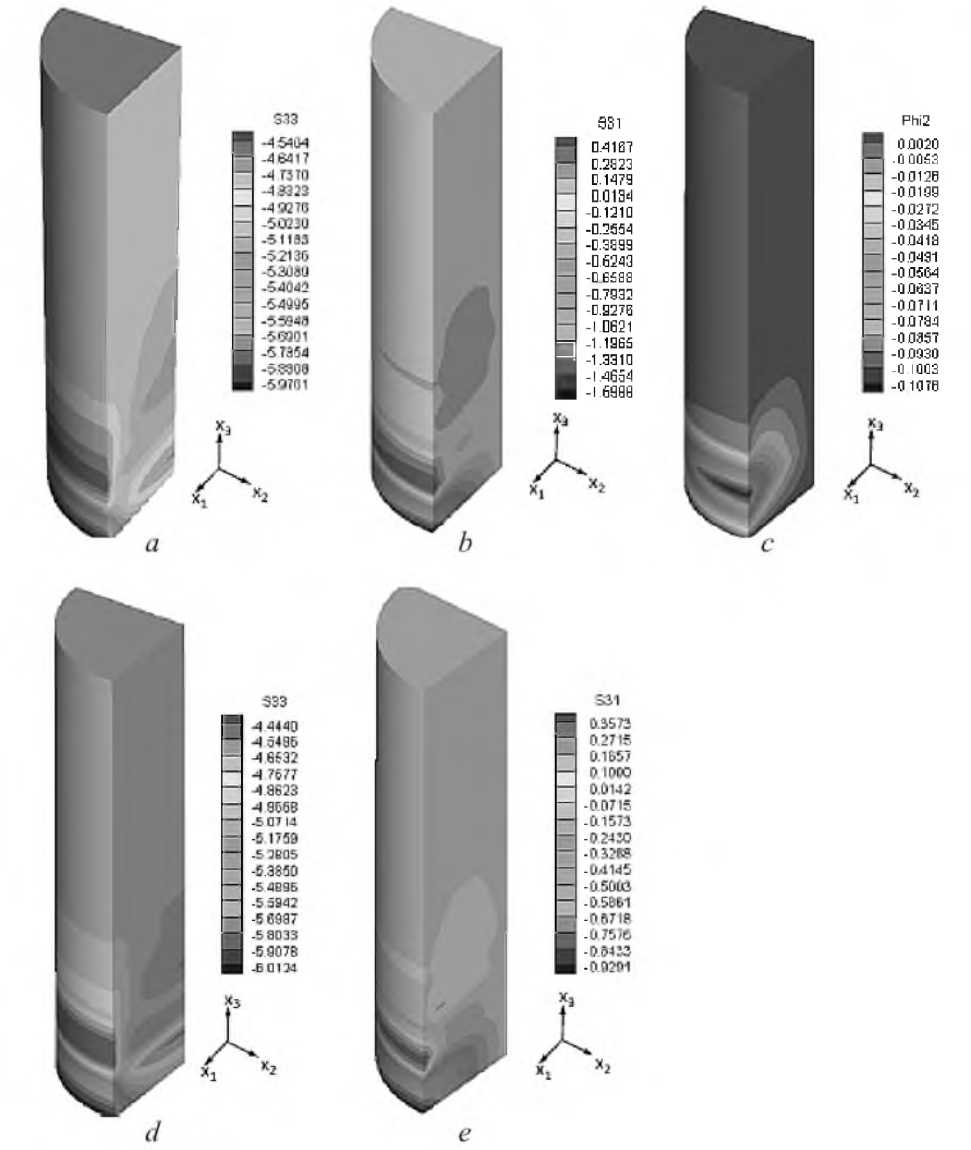

Fig. 5. Typical stress distribution for M2 in MPa and microrotation distribution in degree for applied compressive loading ($\sigma_0 = 5$ MPa): (*a*) micropolar results, σ_{33} ($N = 0.7$); (*b*) micropolar results, σ_{31} ($N = 0.7$); (*c*) micropolar results, φ_2 ($N = 0.7$); (*d*) Cauchy results, σ_{33}; (*e*) Cauchy results, σ_{31}.

The numerical results of the micro- and macrorotation values on M1 (glass) an M2 (rock) are depicted using various coupling numbers N in Fig. 7. Hence, we take into account the convergent solutions for M1 and M2, which contain nano- and microscale pores. As illustrated in Fig. 7, the microrotation and macrorotations have the same behavior.

It can be also concluded that the micro- and macrorotation values are dependent on the pore size, i.e., the M1 (glass, $l_G = 1$ nm) is less depended on micro- and macrorotation than M2 (rock, $l_G = 5$ μm). Furthermore, the coupling number increase results in the micropolar shear constant (κ) increase.

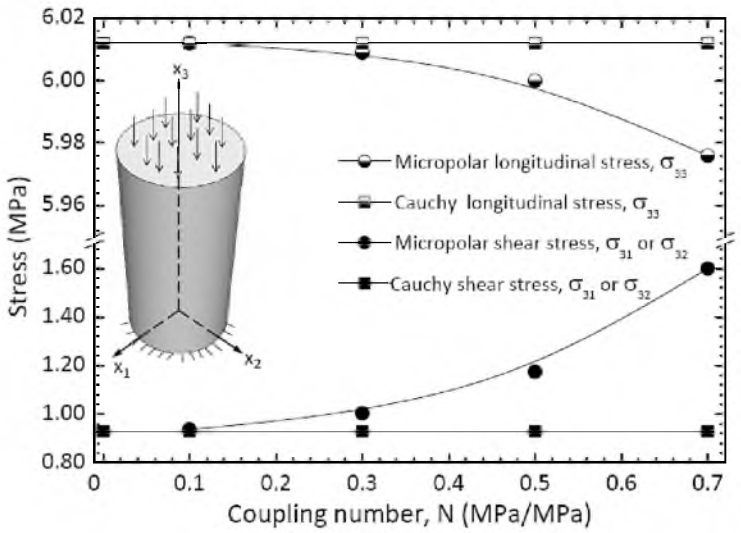

Fig. 6. Presentation of the effect of the coupling number on the axial and shear stress variation in micropolar theory.

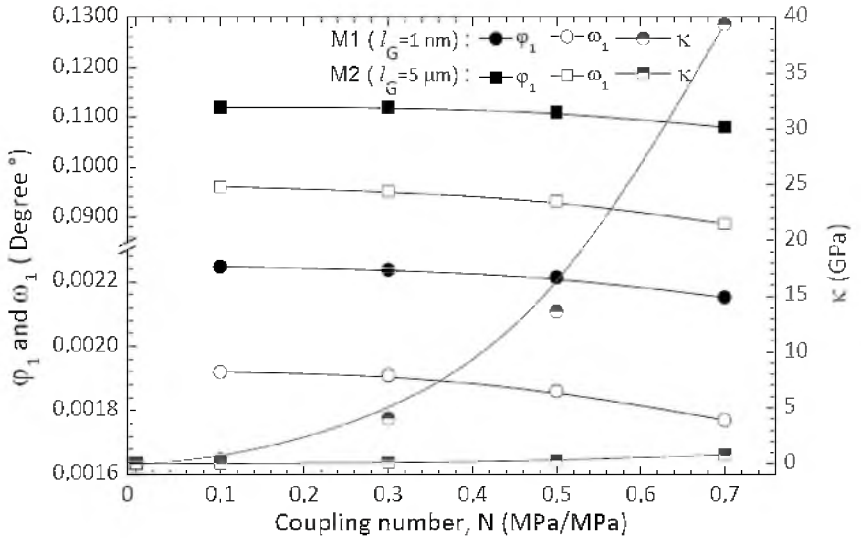

Fig. 7. Effect of the microrotation on the coupling number value N for M1 and M2 materials and variation of micropolar shear constant (κ).

According to the obtained results, the micropolar theory application to the porous materials including the characteristic length (l_G) is restricted to the nano- and microscale, not mesoscale. It is necessary to emphasize that the divergency of solution or converged discontinuous stress fields for M3 and M4 can be obtained.

The numerical result for M3 is shown in Fig. 8 (coupling number is equal to 0.5). In fact, we obtained the axial and shear stress which are the same for both M3 and M4, and discontinuous stress distribution from $N = 0.1$ to 0.5. However, the stress and shear stress distribution is continuous when $N = 0.7$ but these values are the same for both M3 and M4. Hence, for the mesoscale pores, another parameter is required and the solutions are not correct and/or not convergent.

Consequently, such numerical divergences arise from the lack of voids' impacts on the utilized mathematical formulation. To overcome these numerical discrepancies, the pore size and voids should be considered and implemented together [37].

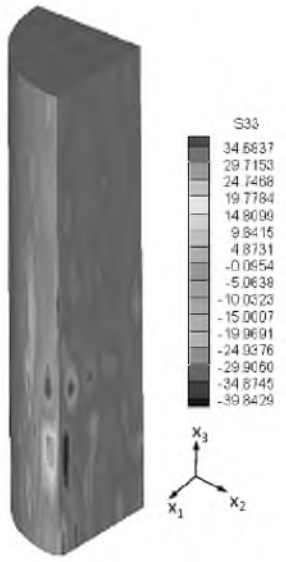

Fig. 8. Typical discontinuous stress distribution for lightweight concrete M3 ($N = 0.5$).

Conclusions. The 3D simulations based on the micropolar theory have been performed on different elastic isotropic brittle materials. The characteristic length (l_G) is considered as the average pore diameter and it is used to obtain α, β, and γ. This assumption leads to a constant polar ratio ($\Psi = 2/3$), so it cannot be accounted for as material constant. By taking advantage of the numerically feasible upper and lower bounds for coupling number ($0.1 \leq N \leq 0.7$), it was found that the coupling number promote the micropolar effects relative to the Cauchy's media. As pointed out before, the micropolar shear constant (κ) depends on the coupling number (Fig. 7). Thus, it is concluded that this value is a material constant. This result is contrary to the recent work [2]. It is believed that the characteristic length scale assumption [Eq. (16)] causes the above conclusion. The comparison material constants, which are extracted in the present paper and [2] substantiates that the presence of a non-material constant is unavoidable. This parameter can be the polar ratio ($\Psi = 2/3$) due to the applied postulates for the characteristic length scales [Eq. (16)], whereas it can be considered as the micropolar shear constant κ, if we take into account the three stress-based material constants [2].

According to the numerical results obtained and comparison between Cauchy's theory and micropolar theory, it can be inferred that the linear elastic isotropic micropolar theory is able to handle the heterogeneous materials including nano- and microscale pores, whereas it results in some physical and numerical drawbacks for the heterogeneous materials with mesoscale pores, e.g., lightweight concretes. Therefore, for the analysis of these kinds of materials (mesoscale pores), it is necessary to take into consideration the voids' impact on the numerical models. For such a methodology, the time-rate constitutive laws and

voids' ratio variations as a time-dependent parameter should be simultaneously taken into account, so that strain localizations, rupture planes and shear band thickness can be numerically extracted via micropolar theory including plasticity aspects.

Резюме

У рамках тривимірної мікрополярної теорії виконано числове моделювання крихких ізотропних матеріалів із різними розмірами пор (аморфне скло, крихка скальна порода і два різних типи легкого бетону) за допомогою циліндричної моделі при дії одновісного стискального навантаження. Для розв'язку задачі припускається, що перша, друга і третя константи мікрообертання (α, β і γ) у рівнянні балансу напружень пропорціональні квадрату середнього діаметра пори або так званої характерної довжини. Показано, що таке припущення приводить до сталості полярного коефіцієнта Ψ і відповідно він не може трактуватися як константа матеріалу. Це може слугувати основою для введення додаткової константи матеріалу для тривимірних мікрополярних середовищ. Відповідно константа мікрополярного зсуву κ є константою матеріалу, що суперечить новим результатам. Виконано числові розрахунки для різних значень степеней вільності N і відповідних областей з метою дослідження характерних особливостей константи мікрополярного зсуву κ. Із використанням запропонованої методики установлено хорошу збіжність та сумісність отриманих даних з експериментальними для різнорідних і однорідних матеріалів із нано- і мікропорами, в той час як для пор мезомасштаба отримано ряд переривчастих або неперетворюваних полів напружень.

1. E. Cosserat and F. Cosserat, *Théorie des Corps Déformables*, Hermann et Fils, Paris (1909).
2. P. Neff, "The Cosserat couple modulus for continuous solids is zero viz the linearized Cauchy-stress tensor symmetric," *ZAMM*, **86**, No. 11, 892–912 (2006).
3. A. C. Eringen and E. S. Suhubil, "Nonlinear theory of simple microelastic solids," *Int. J. Eng. Sci.*, **2**, 189–203 (1964).
4. A. C. Eringen and E. S. Suhubil, "Nonlinear theory of simple microelastic solids," *Int. J. Eng. Sci.*, **2**, 389–404 (1964).
5. A. C. Eringen, "Linear theory of micropolar elasticity," *J. Math. Mech.*, **15**, No. 6 (1966).
6. A. C. Eringen, "Simple microfluids," *Int. J. Eng. Sci.*, **2**, 205–217 (1964).
7. R. D. Midlin and H. F. Tiersten, "Effects of couple stresses in linear elasticity," *Arch. Rat. Mech. Anal.*, **11**, 415–447 (1962).
8. R. A. Toupin, "Elastic materials with couple stresses," *Arch. Rat. Mech. Anal.*, **11**, 385–413 (1962).
9. R. A. Toupin, "Theory of elasticity with couple stresses," *Arch. Rat. Mech. Anal.*, **11**, 85–112 (1964).

10. R. S. Lakes, "Experimental microelasticity of two porous solids," *Int. I. Solids Struct.*, **22**, 55–63 (1985).
11. R. S. Lakes, "A pathological example in micropolar elasticity," *ASME J Appl. Mech.*, **52**, 234–235 (1985).
12. R. S. Lakes, "Size effect due to Cosserat elasticity and surface damage in closed-cell polymethacrylimide foam," *J. Mater. Sci.*, **29**, 6413–6419 (1994).
13. R. S. Lakes, "Experimental methods for study of Cosserat elastic solids and other generalized elastic continua," in: H. B. Mühlhaus (Ed.), *Continuum Models for Materials with Microstructure*, Wiley (1995), pp. 1–25.
14. M. H. Sadd, *Elasticity: Theory, Application, and Numerics*, Butterworth-Heinemann, Elsevier (2005), p. 388.
15. I. Vardoulakis, "Shear-banding and liquefaction in granular materials on the basis of a Cosserat continuum theory," *Ing.-Arch.*, **59**, 106–114 (1989).
16. C. Tekoglu, *Size Effect in Cellular Solids*, PhD Thesis, Rijksunivesiteit Groningen, Netherlands (2007).
17. I. Alsaleh Mustafa, *Numerical Modeling of Strain Localization in Granular Materials Using Cosserat Theory Enhanced with Fabric Properties*, PhD Thesis, Louisiana State University and Agricultural and Mechanical College (2004).
18. Gengkai Hu, Xiaoning Liu, and Tian Jian Lu, "A variational method for nonlinear micropolar composites," *Mech. Mater.*, **37**, 407–425 (2005).
19. J. P. Bardet and J. Proubet, "A numerical investigation of the structure of persistent shear bands in granular media," *Géotechnique*, **41**, No. 4, 599–613 (1992).
20. J. P. Bardet and J. Proubet, "A shear band analysis in idealized granular materials," *J. Eng. Mech., ASCE*, **118**, No. 2, 397–415 (1992).
21. J. Desrues, *Localisation de la Deformation Plastique dans les Matériaux Granulaires*, PhD Thése, Université de Grenoble (1984).
22. Z. P Bazant and G. Pijaudier-Cabot, "Measurement of characteristic length of non local continuum," *J. Eng. Mech., ASCE*, **115**, 755–767 (1989).
23. Z. P. Bazant, "Size effect in blunt fracture; concrete, rock, metal," *J. Eng. Mech., ASCE*, **110**, 518–535 (1984).
24. G. Pijaudier-Cabot and Z. P. Bazant, "Nonlocal damage theory," *J. Eng. Mech., ASCE*, **113**, No. 10, 1512–1533 (1987).
25. R. Pegon, A. R. De Borst, W. Brekelmans, and M. Geers, "Localization issues in local and nonlocal continuum approaches to fracture," *Europ. J Mech. Solids*, **21**, 175–189 (2002).
26. K. Miled, R. Le Roy, K. Sab, and C. Boulay, "Compressive behavior of an idealized EPS lightweight concrete: size effects and failure mode," *Mech. Mater.*, **36**, 1031–1046 (2004).
27. R. D. Gautier, "Experimental investigations on micropolar media," in: *Mechanics of Micropolar Media*, World Scienctific, CISM Lectures, Singapore, (1975), pp. 395–462.

28. R. D. Gautier, et al., "A quest for micropolar constants," *ASME J. Appl. Mech.*, **42**, 396–374 (1975).

29. R. D. Gautier, et al., "Bending of a curved bar of micropolar elastic material," *ASME J. Appl. Mech.*, **43**, 502–503 (1976).

30. J. Jeong, H. Adib-Ramezani, and M. Al-Mukhtar, "Application of a novel micropolar media to the brittle materials: role of porosity and characteristic length," NUMOG X (Tenth Int. Symp. on *Numerical Models in Geomechanics*), Greece, 25–27 April, 2007.

31. J. Jeong, H. Adib, and G. Pluvinage, "Proposal of new damage model for thermal shock based on dynamic fracture on the brittle materials," *J. Non-Crystalline Solids*, **351**, 2065–2075 (2005).

32. K. Beck, *Étude des Propriétés Hydriques et des Mécanismes d'Altération de Pierres Calcaires à Forte Porosité*, PhD Thése, Université d'Orléans, France (2006).

33. K. Haidar, *Damage Modeling of Concrete Structures-Numerical Approaches and Microstructure Effects on the Rupture Properties*, PhD Thesis, Nantes University, France (2002).

34. J. H. Heinbockel, *Introduction to Tensor Calculus and Continuum Mechanics*, Trafford Publishing (2001).

35. R. S. Lakes, "Experimental methods for study of Cosserat elastic solids and other generalized elastic continua," in: H. Mühlhaus and J. Wiley (Eds.), *Continuum Models for Materials with Microstructure*, New York (1995), Ch. 1, pp. 1–22.

36. D. Bigoni and W. J. Drugan, "Analytical derivation of Cosserat moduli via homogenization of heterogeneous elastic materials," *J. Appl. Mech.*, **74**, 741–753, (2007).

37. Wenxing Haung and E. Bauer, "Numerical investigations of shear localization in a micropolar hypoplastic material," *Int. J. Num. Anal. Meth. Geomech.*, **27,** 325–352 (2003).

Received 09. 10. 2007